Germanium/silicon ratios in the Copper River Basin, Alaska: Weathering and partitioning in periglacial versus glacial environments

Alison M. Anders,[1] Ronald S. Sletten,[2] Louis A. Derry,[3] and Bernard Hallet[2]

[1] Glacial to interglacial variation in the germanium to silicon ratio (Ge/Si) of biogenic opal in oceanic sediment cores has been proposed to record terrestrial silicate weathering intensity. However, data connecting Ge/Si ratios to weathering are sparse, especially for cold regions. To characterize Ge/Si of the dissolved loads of rivers draining modern glacial and periglacial regions, we measured Ge and major element chemistry of more than 30 streams in the Copper River Basin of south Alaska. We measured significantly higher Ge/Si in rivers with greater than 15% glacial cover in their basins than in rivers draining areas with less glacial cover, which we attribute to preferencial subglacial weathering of biotite. We also ran laboratory experiments to investigate the role of differential sorption of Ge and Si on hydrous iron oxides in moderating the Ge/Si ratio of rivers in recently deglaciated basins. These experiments indicate that Ge is preferentially adsorbed over Si by hydrous iron oxides over a wide range of pH values and support differential sorption as a potentially significant fractionation process. Our measured high Ge/Si in glaciated basins is in striking contrast to the low Ge/Si in the oceanic record during glacial periods. The glacial to interglacial changes in marine Ge/Si cannot simply reflect changes in glacier cover on land, as the mineralogy of silicates weathered and processes partitioning Ge in soils must also strongly influence the fluvial Ge and Si inputs to the ocean.   *INDEX TERMS:* 1030 Geochemistry: Geochemical cycles (0330); 1065 Geochemistry: Trace elements (3670); 1806 Hydrology: Chemistry of fresh water; 1871 Hydrology: Surface water quality; *KEYWORDS:* chemical weathering, germanium, silicon, glacial, periglacial

1. Introduction

[2] The Quaternary is characterized by periodic transitions between glacial and interglacial climates that can be detected in geomorphic, sedimentological, biological, and chemical paleoclimate records around the globe. Quaternary marine records of the germanium to silicon ratio (Ge/Si) of biogenic opal in sediment cores show significant changes that occur in phase with changes in global ice volume and atmospheric CO_2 levels [*Froelich et al.*, 1992]. The questions we address are (1) how do fluvial Ge/Si ratios from glaciated and periglacial basins compare to one another and to those from other world rivers and (2) what mechanisms control these Ge/Si ratios. Assessment of the effect of glacial and periglacial processes on fluvial Ge/Si will allow for better interpretation of global fluvial Ge/Si through time and its impact on marine Ge/Si.

[1]Department of Earth and Space Sciences, University of Washington, Seattle, WA, USA.
[2]Quaternary Research Center, University of Washington, Seattle, WA, USA.
[3]Department of Earth and Atmospheric Sciences, Cornell University, Ithaca, NY, USA.

[3] Ge is a trace element that behaves similarly to Si in geochemical processes, substituting for Si in the lattices of silicate minerals at an average crustal concentration of 1.5 ppm [*Burton et al.*, 1959; *Bernstein*, 1985]. Dissolved Ge is supplied to the ocean via fluvial and groundwater transport, hydrothermal alteration of the seafloor and the dissolution of wind-blown dust in the ocean. These different sources of Ge have distinct Ge/Si signatures [*King et al.*, 2000]. The average river Ge/Si is 0.54 μmol/mol, and rivers supply an estimated 70% of Ge to the ocean [*Froelich et al.*, 1992]. Hydrothermal alteration of seafloor basalt adds Ge at a Ge/Si ratio of about 7 μmol/mol [*Mortlock et al.*, 1993]. Groundwater and dust fluxes to the ocean are more difficult to quantify, both in terms of Ge/Si and absolute mass transport. Aeolian material is expected to be enriched in Ge/Si relative to continental crust because of the observed high Ge/Si of soils [*Munhoven and Francois*, 1996]. However, during glacial periods the source of dust may shift from soils to primary mineral fragments derived from glacial grinding. *Kurtz* [2000] found that dust-derived pelagic sediments are enriched in Ge/Si and depleted in Si/Al relative to loess – indicating that once dust reached the ocean, some Si and Ge was dissolved and contributed Ge to the ocean at a low Ge/Si. Siliceous-shelled animals take up Ge without significant fractionation and biogenic

opal derived from these shells provides a major sink of Ge in the ocean [*Froelich et al.*, 1992]. An additional sink of Ge is necessary to balance the global Ge budget [*Zhou and Kyte*, 1991; *Elderfield and Schultz*, 1996]. A sedimentary sink of Ge in addition to opal is proposed based on profiles of Ge, Fe, and Si in sediments off the California margin [*Hammond et al.*, 2000] and the Antarctic South Atlantic [*King et al.*, 2000]. In both regions, sequestered Ge is associated with Fe in cores that are experiencing opal dissolution, indicating that early diagenesis of diatoms may decouple Ge from Si and provide the "missing sink" of Ge [*King et al.*, 2000; *Hammond et al.*, 2000].

[4] Changes in the flux or Ge/Si ratio of any of the sources or sinks could influence the Ge/Si ratio of the ocean through glacial to interglacial climates. However, climate-induced changes in the flux and the Ge/Si ratio of the global fluvial contribution of dissolved material are the prevailing explanations for the observed variations in opal Ge/Si ratio [*Froelich et al.*, 1992, *Munhoven and Francois*, 1996]. Yet, little is known about the direct impact of glaciation on terrestrial Ge and Si cycles, limiting the interpretation of marine Ge/Si in terms of terrestrial environmental change.

[5] In river waters, Ge occurs at levels of about 100 pmol/L and dissolved Ge/Si ratios are almost always lower than those of the bedrock being drained [*Froelich et al.*, 1992]. The low fluvial ratio implies that Ge is sequestered in the solid phases relative to Si during rock weathering [*Murnane and Stallard*, 1990]. Mechanisms for retaining Ge in the solid phases include incorporation in secondary aluminosilicate minerals and sorption on or precipitation with iron oxides. *Murnane and Stallard* [1990] measured Ge/Si ratios about 2.5 times that of parent bedrock in three tropical soils and suggested that the preferential accumulation of Ge in clay minerals was the mechanism leading to this enrichment. The second proposed mechanism of Ge sequestration, precipitation on iron oxides, finds support in the fact that Ge was originally measured by coprecipitation with hydrous iron oxide [*Burton et al.*, 1959]. In addition, goethite, an iron oxide, has been observed to have concentrations of hundreds to thousands of ppm Ge [*Bernstein*, 1985; *Bernstein and Waychunas*, 1987]. *Mortlock and Froelich* [1987] conjectured that anomalously low Ge/Si ratios could be due to sorption on hydrous iron hydroxide surfaces. However, *Chillrud et al.* [1994] found evidence for significant concentrations of freshly precipitated iron hydroxides on the suspended sediment of a glacial stream in the Andes that also had a high dissolved Ge/Si ratio. In tropical weathering environments, *Kurtz et al.* [2002], have shown that formation of Ge-enriched secondary alumino-silicate phases is the largest source of Ge/Si fractionation in soils. However, they also found that Ge/Si is enriched in extractable Fe-oxide fractions, although these contribute substantially less to the overall weathering mass balance in the system studied.

[6] Silicate weathering in the near surface is not the sole source of Ge to the dissolved load of rivers; hydrothermal waters, coal fly ash, and weathering of sulfide minerals can also contribute Ge to rivers. Hot springs are often enriched in germanium relative to silicon, exhibiting Ge/Si ratios up to 1000 μmol/mol, 3–4 orders of magnitude higher than average rivers and may have such high concentrations of Ge that a small volumetric contribution of hydrothermal water can dominate the Ge/Si of a river [*Arnorsson*, 1984; *Criaud*

and *Fouillac*, 1986; *Evans and Derry*, 2002]. Fly ash from coal combustion also has an extremely high Ge/Si ratio, swamping the natural Ge/Si in many rivers in populated areas [*Froelich et al.*, 1985, 1992]. The oxidation of sulfide minerals is another potential nonsilicate source of Ge since sulfide ores can be greatly enriched in Ge [*Bernstein*, 1985].

2. Study Area

[7] The Copper River Basin of central Alaska was chosen as the field area because it permits easy sampling of glacial and periglacial rivers in four different regions: the Wrangell Mountains, Alaska Range, Chugach Mountains, and the Copper Basin Interior (Figure 1 and Table 1). The Wrangell Mountains are in the Wrangellia Terrane; the dominant lithologies in this area are basalt, limestone, sandstone, marine clastics and volcaniclastics, and minor granitic plutons [*Nokleberg et al.*, 1994]. The eastern end of the Alaska Range is partially within the Wrangellia Terrane and contains many of the same formations. The central Alaska Range is dominantly composed of three metamorphic sequences including pelitic schist, calcite and dolomite marble, and schistose diorite. The Chugach Mountains are also partially within the Wrangellia Terrane with deeper levels exposed including the basement metagranite and metadiorite [*Nokleberg et al.*, 1994]. The Peninsular Terrane, which is composed of a metamorphic mafic-ultramafic basement, the granitic Alaska-Aleutian Range Batholith, and a marine calcareous and volcanic sequence comprise the rest of the Chugach Mountains [*Nokleberg et al.*, 1994]. The interior of the Copper River basin is underlain by the Wrangellia and Peninsular Terrains and covered by a sequence of fluvial, glacial, and lacustrine deposits and andesitic lavas [*Nokleberg et al.*, 1994].

[8] The river basins sampled are arbitrarily defined as glaciated if 15% or more of their areas are ice covered; all other basins sampled are considered periglacial. The discharge, basin area, and geomorphology of rivers vary considerably within both the glacial and periglacial groups. Glaciated basins are larger than periglacial basins (averaging ~4000 km^2 versus 400 km^2), but there is overlap: glacial basins ranged from about 315 km^2 to the entire Copper River basin at about 52,000 km^2, whereas periglacial basins sampled were between 2 km^2 and 3000 km^2. Glacial rivers all have their headwaters in mountainous regions, although many had significant input from lower relief regions as well. Both steep, mountainous basins and lowland basins were included in the periglacial group. All the large periglacial basins are in the low-lying interior region. The timing of annual peaks in discharge varies with the geomorphology of the basins. Mean monthly discharge from Squirrel Creek, a lowland, periglacial stream is highest in May, while the Little Tonsina River, a periglacial mountain stream and the glacial Tonsina River have their highest mean monthly discharge in June or July [*Emery et al.*, 1985]. The stage was high to very high in all the rivers at the time of sampling (July 2000) due to heavy rains.

[9] The remote Copper River Basin is likely to be free of contamination by fly ash from coal combustion. However, there are coal beds in the central Copper River Basin that could contribute locally to the dissolved load of rivers in the study area [*Motyka et al.*, 1989]. In addition, there is
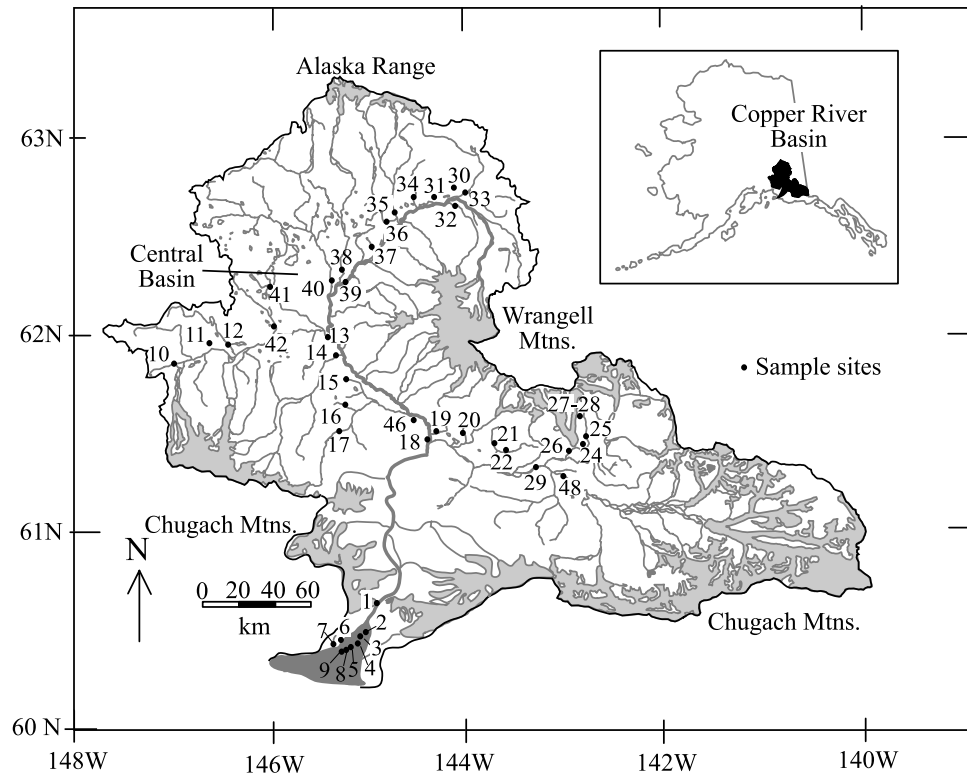
Figure 1. The Copper River Basin of south central Alaska. Inset map of Alaska shows the location of the Copper River Basin. Geographic regions are named and glacial cover is indicated by gray shading. The main stem of the Copper River is shown as a bold gray line; tributaries are in thinner gray lines. Water and suspended sediment samples were taken at each of the numbered sample sites.

hydrothermal activity in the region that could alter to the chemistry of rivers: a number of hot springs have been mapped in the central Copper River Basin [*Miller*, 1994]. Oxidation of sulfide minerals is a potential source of Ge since the late Tertiary volcanic rocks of the Wrangell Mountains host sulfide-rich vein deposits of copper ores, giving the Copper River its name [*Bateman and McLaughlin*, 1920].

3. Methods

[10] Water samples, filtered at 0.45 μm, were taken from 37 sites within the Copper River Basin including five sites along the main stem of the Copper River and both glacial and periglacial tributaries of the Copper River and the Matanuska River in a neighboring basin (Figure 1 and Table 1). The Ge and major element chemistry was measured in order to determine the Ge/Si ratio of the dissolved load of these rivers and to identify the relationship between Ge concentrations, Ge/Si, and the chemistry of the dissolved load. Major cations (Al^{3+}, Ca^{2+}, K^+, Na^+, Fe^{2+}, Mg^{2+}, Mn^{2+}, Si^+) were measured in subsamples acidified with 0.1M HCl using a Jarrel-Ash 755 ICP-AES (inductively coupled plasma atomic emission spectroscopy) at the University of Washington's Chemistry Department. The error in measurement was less than 2% for Mg, K, and Ca, less than 5% for Na and Si, and less than 15% for Al, Fe, and Mn, which were present in very low concentrations. Major anions (Cl^-, Br^-, SO_4^-, PO_4^-, NO_3^-) were measured by ion chromatography in the

University of Washington's College of Forest Resources with errors of <2%. The trace element Ge was measured by isotope dilution, hydride generation ICP-MS [*Mortlock and Froelich*, 1996] using a continuous flow hydride generator interfaced with a Finnigan Element 2 ICP-MS in the Department of Earth and Atmospheric Sciences, Cornell University. Uncertainties in Ge concentrations, including blank corrections, are less than 3% using this system [*Evans and Derry*, 2002]. Suspended sediment samples from 19 locations were dissolved by fusing at 900°C with lithium metaborate and then dissolving with HNO_3. Major cations and Ge were measured in these samples after dilution, as above, with uncertainties <2%.

[11] A laboratory experiment was designed to investigate the differential sorption of Ge and Si on poorly crystalline iron oxides following the method described by *Blum* [1998]. First, $Fe(OH)_3 \cdot nH_2O$ was precipitated by raising the pH to 9 of a solution of 0.01M $Fe_2(SO_4)_3$ and 0.1 $NaNO_3$ [*Dzombak and Morel*, 1990]. The precipitate was stirred overnight at room temperature and subsamples were taken and adjusted to pH 4, 5, 6, 7, 8, and 9. The total Fe concentration in the samples was about 35 mg/L. Ge and Si were added to the precipitated poorly crystalline, hydrous iron oxide at a Ge/Si ratio of 2 μmol/mol with Si at 10 ppm. These concentrations of Ge and Si were selected to mimic concentrations in rivers. Samples were then agitated for 24 hours and split. One part of each sample was acidified to pH 4 to dissolve hydrous iron oxide and total Ge, Si, and Fe were measured. The other sample split was filtered at 0.45 μm and the pH

Table 1. Water Sample Site Description

Site	Site Name	Region	Type	Latitude	Longitude	Date	Time,[a]UT	Sediment Concentration, g/L	pH
1-A	Childs Glacier	entire basin	glacial	60°39.5′	144°46.0′	08	1530	0.43	8.27
1-B	Childs Glacier	entire basin	glacial	60°39.5′	144°46.0′	09	800	0.56	8.24
1-C	Childs Glacier	entire basin	glacial	60°39.5′	144°46.0′	09	1810	0.60	7.87
2	Hotcakes	entire basin	glacial	60°31.3′	144°49.9′	09	1030	0.75	8.30
3	Long Island	entire basin	glacial	60°29.2′	144°58.0′	09	1130	0.68	8.31
4	Delta Backwater	entire basin	glacial	60°29.0′	144°59.1′	09	1200	0.45	8.39
5	Flag Point	entire basin	glacial	60°26.7′	145°2.2′	09	1240	078	8.30
6	Alaganik Slough	Chugach Mountains	glacial	60°27.1′	145°13.7′	09	1400	0.01	7.07
7	Sheridan River	Chugach Mountains	glacial	60°28.4′	145°23.1′	09	1430	0.07	6.94
8	Western Delta	Entire basin	glacial	60°27.0′	145°4.2′	09	1600	0.73	8.27
9	West Delta	Entire basin	glacial	60°27.0′	145°3.9′	09	1630	0.64	8.00
10	Little Nelchina	Chugach Mountains	periglacial	61°59.4′	146°56.8′	11	1130	0.19	8.01
11	Mud Springs	Interior	spring	62°06.8′	145° 58.6′	11		0.20	7.04
12	Tolsona Creek	Interior	periglacial	62°06.8′	145°58.6′	11		0.02	8.01
13	Tazlina Creek	Chugach Mountains	glacial	62°03.2′	145°25.6′	12	1000	0.41	7.95
14	Klutina River	Chugach Mountains	glacial	61°57.2′	145°18.5	12	1100	0.34	7.93
15	Willow Creek	Chugach Mountains	periglacial	61°49.0′	145°12.9′	12	1145	0.02	7.90
16	Squirrel Creek	Chugach Mountains	periglacial	61°40.0′	145°10.6′	12	1300	0.03	7.96
17	Tonsina River	Chugach Mountains	glacial	61°39.0′	144°39.2′	12	1400	0.09	7.83
18[b]	Copper River at Chitina	most of the basin	glacial	61°31.8′	144°24.5′	12	1530	0.81	8.09
19	Kotsina River	Alaska Range	glacial	61°32.3′	144°22.6	12	1600	1.46	8.11
20	Strelna Creek	Alaska Range	periglacial	61°30.6′	144°04.1′	13	1100	0.02	8.16
21	Choksona River	Alaska Range	periglacial	61°27.3′	143°45.8′	13	1230	0.02	8.17
22	Gilahina River	Alaska Range	periglacial	61°26.3′	143°43.2′	13	1300	0.02	8.03
23	Lakina River	Alaska Range	glacial	61°22.5′	143°20.9′	13	1400	0.12	8.06
24-A	Clear Creek	Wrangell Mountains	spring	61°26.1′	143°25.6′	13	1800	0.02	7.65
24-B	Clear Creek	Wrangell Mountains	spring	61°26.1′	143°25.6′	15	1300	0.01	7.89
25-A	Kennicott River	Wrangell Mountains	glacial	61°26.0′	142°56.6′	13	1745	0.50	8.40
25-B	Kennicott River	Wrangell Mountains	glacial	61°26.0′	142°56.6′	14	0845	0.50	8.25
25-C	Kennicott River	Wrangell Mountains	glacial	61°26.0′	142°56.6′	14	1245	0.50	8.44
25-D	Kennicott River	Wrangell Mountains	glacial	61°26.0′	142°56.6′	14	1630	0.37	8.51
25-E	Kennicott River	Wrangell Mountains	glacial	61°26.0′	142°56.6′	14	2100	0.58	8.48
25-F	Kennicott River	Wrangell Mountains	glacial	61°26.0′	142°56.6′	15	1100	0.63	8.62
25-G	Kennicott River	Wrangell Mountains	glacial	61°26.0′	142°56.6′	15	1530	0.55	8.59
26-A	McCarthy Creek	Wrangell Mountains	periglacial	61°25.9′	142°55.6′	14	1100	0.06	8.06
26-B	McCarthy Creek	Wrangell Mountains	periglacial	61°25.8′	142°54.9′	14	1445	0.07	8.25
26-C	McCarthy Creek	Wrangell Mountains	periglacial	61°25.9′	142°55.6′	14	2045	0.04	8.19
26-D	McCarthy Creek	Wrangell Mountains	periglacial	61°25.9′	142°55.6′	15	1000	0.05	7.96
26-E	McCarthy Creek	Wrangell Mountains	periglacial	61°25.9′	142°55.6′	15	1600	0.05	8.33
26-F	McCarthy Creek	Wrangell Mountains	periglacial	61°25.9′	142°55.6′	16	0900	0.09	7.89
27	Jumbo Creek	Wrangell Mountains	periglacial	61°30.3′	142°52.4′	14	1700	0.00	8.17
28	Bonanza Creek	Wrangell Mountains	periglacial	61°31.0′	142°54.1′	14	1800	0.01	8.16
29	Chitina River	Chugach Mountains	glacial	61°20.9′	143°12.8′	15	1800	1.96	8.24
30	Porcupine Creek	Alaska Range	periglacial	62°43.7	143°52.3′	16	1900	0.02	8.07
31	Athell Creek	Alaska Range	periglacial	62°43.1′	143°57.8′	17	0830	0.01	7.65
32	Copper River at Slana	Wrangell Mountains	glacial	62°42.2′	143°56.8′	17	0930	0.20	7.97
33	Slana River	Alaska Range	glacial	62°51.4′	143°42.8′	17	1020	0.17	8.11
34	Indian Creek	Alaska Range	periglacial	62°40.0′	144°25.6′	17	1100	0.03	7.88
35	Chistochina River	Alaska Range	glacial	62°36.0′	144°38.7′	17	1200	1.97	8.13
36	Sinona Creek	Interior	periglacial	62°35.5′	144°38.9′	17	1300	0.00	7.98
37	Tulsona River	Interior	periglacial	62°25.8′	144°57.9′	17	1345	0.01	8.16
38	Gakona River	Alaska Range	glacial	62°18.1′	145°18.2′	17	1430	1.85	8.19
39	Copper River at Gakona	Wrangell Mountains	glacial	62°18.5′	145°13.9′	17	1530	0.77	8.10
40	Gulkana River	Interior	periglacial	62°16.2′	145°23.3′	17	1600	0.01	8.12
41	Lake Louise	Interior	periglacial	62°17.1′	146°32.4′	18	1230	0.00	7.75
42	Mendeltna River	Interior	periglacial	62°02.9′	146°32.7′	18	1400	0.01	8.17
43-A1	Matanuska	Chugach Mountains	glacial	61°46.5′	147°46.0′	20		0.88	8.40
43-A2	Matanuska	Chugach Mountains	glacial	61°46.5′	147°46.0′	21		1.09	8.22
43-B	Matanuska	Chugach Mountains	glacial	61°46.5′	147°45.7′	20		0.57	8.26
43-C	Matanuska	Chugach Mountains	glacial	61°46.6′	147°45.6′	20		0.65	8.30
43-D	Matanuska	Chugach Mountains	glacial	61°46.9′	147°46.3′	20		0.51	8.39
43-E	Matanuska	Chugach Mountains	glacial	61°47.1′	147°44.0′	21	1130	0.62	8.10
43-F	Matanuska	Chugach Mountains	glacial	61°47.1′	147°47.1′	21	1330	0.70	8.00
44	Matanuska	Chugach Mountains	glacial	61°46.7′	148°28.5′	21		0.38	8.06
45	Hick's Creek	Chugach Mountains	glacial	61°47.6′	147°56.1′	21		0.38	8.31
46	Liberty Creek	Chugach Mountains	periglacial	61°37.3′	144°32.9′	13	1800	0.01	7.74
47	Clear Creek	Wrangell Mountains	spring	61°25.7′	143°36.0′	15	1300	0.04	7.62
48	Nizina River	Wrangell Mountains	glacial	61°21.4′	143°15.1′	15	1800	0.67	8.21

[a]Dates are all during the month of July 2000; time of sampling is not available for all samples.
[b]This sample was taken immediately downstream of the junction of the Copper River and the Kotsina River and mixing between the two appears to be incomplete. This sample is therefore considered to reflect the Kotsina River and is excluded from further analyses.

Table 2. Suspended Sediment Major Elements and Ge/Si

Sample	Site Name	Ge/Si, μmol/mol	Sediment, wt %							
			Al	Ca	Fe	K	Mg	Mn	Na	Si
s-1-A	Childs Glacier	2.15	7.32	3.86	5.51	1.90	2.63	0.12	1.30	17.94
s-1-B	Childs Glacier	3.22	4.46	2.69	3.29	1.06	1.59	0.07	0.84	11.74
s-2	Hotcakes	2.69	6.44	4.21	4.44	1.43	2.17	0.10	1.35	18.03
s-13	Tazlina Creek	2.33	7.89	3.09	5.06	1.92	2.27	0.00	2.10	27.41
s-17	Tonsina River	2.42	5.30	2.11	3.95	0.95	1.94	0.03	0.26	15.81
s-18[a]	Copper River at Chitina	0.89	6.28	2.99	2.93	1.08	1.43	0.06	1.70	19.00
s-19	Kotsina River	1.54	8.29	4.39	3.49	1.73	1.78	0.05	2.69	25.60
s-23	Lakina River	2.13	4.10	7.67	1.93	0.70	1.05	0.03	1.14	15.06
s-25-B	Kennicott River	2.06	6.02	9.64	3.13	1.67	1.74	0.01	1.89	20.10
s-25-D	Kennicott River	2.91	5.05	7.35	2.59	1.19	1.39	0.00	1.35	14.61
s-25-F	Kennicott River	2.51	4.94	8.16	2.45	1.12	1.35	0.01	1.57	15.84
s-26-F	McCarthy Creek	3.92	4.63	3.53	1.91	0.60	1.02	0.00	1.16	13.07
s-26-M	McCarthy Creek	2.80	4.24	3.08	1.91	0.60	1.01	0.00	1.11	12.85
s-33	Slana River	2.36	5.12	1.82	3.03	1.42	1.21	0.00	1.24	22.40
s-39	Copper River at Gakona	1.92	5.29	2.51	2.96	1.20	1.38	0.06	1.47	16.27
s-43-F	Matanuska River	2.87	9.68	1.74	5.73	3.31	2.34	0.07	1.74	24.38
s-44	Matanuska River	2.38	8.66	1.59	5.14	2.70	2.14	0.03	1.75	22.39
s-45	Matanuska River	3.82	8.57	1.89	4.83	2.39	1.93	0.03	1.97	26.48
s-48	Nizina River	3.78	6.46	5.20	3.98	1.36	1.93	0.06	1.83	19.76

[a]This sample was taken immediately downstream of the junction of the Copper River and the Kotsina River, and mixing between the two appears to be incomplete. This sample is therefore considered to reflect the Kotsina River and is excluded from further analyses.

was adjusted to 4; dissolved Ge, Si, and Fe were then measured in this sample by the techniques described for the river dissolved load samples. A control sample was subjected to the same treatment without the addition of Ge or Si, and yielded 0.05 ppm Si and 4 ppt Ge and 38 ppm Fe.

4. Results

[12] Ge/Si ratios in the sediment samples range from 0.89–3.92 μmol/mol (average 2.56, std. dev. = 0.77, n = 19), reflecting a range of crustal sources (Table 2). Most dissolved load samples from the rivers have Ge/Si below the average suspended sediment value. Samples from the periglacial rivers fall on a mixing line for Ge/Si versus 1/[Si] of the form suggested by *Murnane and Stallard* [1990] and are consistent with that found for Alaskan rivers by *Froelich et al.* [1992] (Ge/Si = 58.5 * 1/[Si] − 0.04, versus *Froelich et al.*'s [1992] result, Ge/Si = 58 * 1/[Si] − 0.03) (Figure 2 and Table 3). *Froelich et al.* [1992] have interpreted this kind of relationship as a mixing between a high [Si], low Ge/Si source produced by weathering of primary minerals and a low [Si], high Ge/Si source from dissolution of Ge-enriched secondary clay minerals. Samples from the glacial rivers do not fit a linear trend as well, and suggest that another process is involved in their Ge-Si systematics.

[13] Samples from two rivers clearly deviate from any linear relationship between Ge/Si and 1/[Si]; the Kennicott and Kotsina rivers of the Wrangell Mountains have Ge/Si ratios that are much higher (3.5–11 μmol/mol) than normally found in unpolluted streams. The Ge/Si ratios of the Kennicott and Kotsina rivers are so high that a local mechanism controlling Ge/Si in these two rivers is likely. Such high values in unpolluted streams have only been reported from systems affected by hydrothermal activity [*Mortlock and Froelich*, 1987; *Evans and Derry*, 2001]. Ge concentrations in these rivers increase with the total solute load and are not correlated with the K/Na ratio, as in other glacial rivers. These rivers appear to be impacted by hydrothermal input, or possibly weathering of sulfide minerals which can have high Ge contents [*Bernstein*, 1985]. Both hydrothermal activity

and sulfide mineralization are present in the Wrangell Mountains, and our data do not allow us to distinguish between the two. These rivers are not included in subsequent analyses.
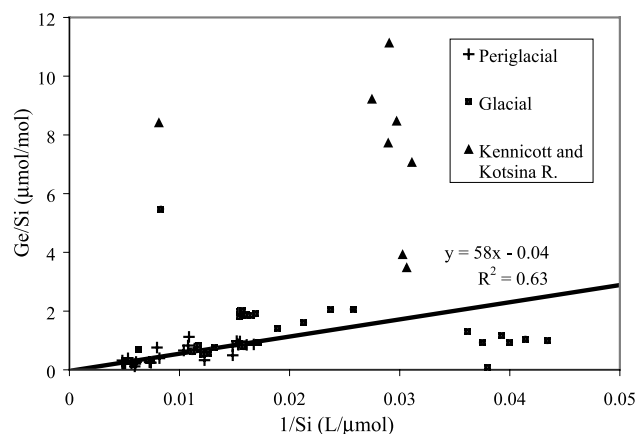
Figure 2. Ge/Si versus 1/Si. The periglacial rivers sampled tend to have lower Ge/Si and higher concentrations of Si than glacial rivers sampled. The Kennicott and Kotsina Rivers have much higher Ge/Si than other rivers sampled and do not lie on any linear array. Such behavior is consistent with small amounts of input from hot springs which typically have very high Ge/Si but variable Si concentration [*Evans and Derry*, 2002]; however, no hot springs have been found despite extensive exploration in this area, and known sulfide-rich deposits may also be the source of the high Ge. The average Ge/Si of glacial rivers (1.42) is noticeably higher than the average Ge/Si of world rivers (0.54) [*Froelich et al.*, 1992]. Regression line fit to periglacial river Ge/Si and 1/[Si] is similar to that of *Froelich et al.* [1992] determined for several Alaskan rivers (Ge/Si = 58 * 1/[Si] − 0.03). Glacial rivers are less well fit by the line, suggesting the presence of another source of variation in Ge/Si.

Table 3. Major Element and Germanium Chemistry

Site	Anions, μmol/L						Cations, μmol/L								Ge, pmol/L	Ge/Si, μmol/mol
	Br	Cl	HCO$_3$	NO$_3$	PO$_4$	SO$_4$	Al	Ca	Fe	K	Mg	Mn	Na	Si		
1-A	–	73.7	1420	6.00	–	181	2.52	477	0.609	56.5	108	0.164	54.5	64.6	116.7	1.80
1-B	–	88.7	1590	7.00	–	175	2.48	462	0.842	58.9	106	0.218	50.4	62.3	118.0	1.89
1-C	0.125	102	1000	9.35	1.00	177	2.11	474	0.734	58.8	107	0.164	52.8	62.7	116.4	1.86
2	–	62.5	2030	7.85	–	176	2.33	457	0.824	53.9	105	0.164	49.7	62.4	116.3	1.86
3	–	51.1	1990	6.07	–	180	2.89	469	0.967	54.6	109	0.182	51.2	64.2	122.6	1.91
4	–	52.3	1520	5.71	0.839	173	1.82	480	0.734	54.6	105	0.182	75.7	60.4	112.2	1.86
5	–	51.3	2810	5.43	–	180	2.22	468	0.895	56.7	109	0.200	52.1	64.8	129.5	2.00
6	–	56.8	765	18.7	0.323	58.4	–	166	1.31	7.67	13.6	0.109	19.2	38.8	80.1	2.06
7	–	44.5	745	7.21	0.807	72.2	1.04	141	1.20	26.8	22.7	0.164	23.1	47.0	75.2	1.60
8	–	53.1	2450	5.71	–	180	2.96	483	1.25	56.2	110	0.182	51.0	64.6	130.5	2.02
9	–	65.2	995	12.0	1.36	180	3.08	479	1.18	55.8	109	0.182	51.6	63.8	128.9	2.02
10	–	37.4	1750	23.8	–	1710	1.56	1411	0.949	27.9	284	0.218	292	126	95.4	0.76
11	439	327000	1730	1020	17.6	34.8	10.0	8170	3.90	2040	1046	30.9	17700	147	5031.7	34.24
12	2.93	1110	1430	7.28	–	23.4	1.85	568	3.49	50.2	207	0.710	262	92.9	76.9	0.83
13	0.213	249	927	6.78	–	195	2.00	509	0.752	18.8	97.3	0.455	91.0	52.8	74.7	1.42
14	0.175	148	831	12.7	–	110	1.52	410	0.788	14.5	74.1	0.364	34.0	58.3	54.0	0.93
15	–	134	2930	5.14	–	35.5	1.52	848	5.17	33.9	380	0.455	93.3	198	43.7	0.22
16	–	136	1130	10.1	0.323	53.1	1.37	410	0.895	17.5	139	0.182	46.4	167	35.4	0.21
17	–	99.1	736	10.9	–	81.1	2.11	345	1.11	10.8	61.3	0.182	26.4	79.4	44.1	0.56
18[a]	0.125	160	1100	8.92	–	294	5.97	573	0.949	38.3	142	0.455	118	120	659.4	5.48
19	0.163	167	1130	9.57	4.13	317	6.45	577	0.967	43.9	133	0.473	145	123	1034.6	8.41
20	–	67.8	2470	16.6	–	2330	1.04	2050	0.394	21.9	555	0.237	130	92.0	103.2	1.12
21	–	74.9	1950	16.8	–	1090	–	1350	0.286	15.1	326	0.164	89.2	87.9	63.9	0.73
22	0.363	365	1440	23.6	–	295	0.593	790	0.376	10.4	141	0.218	50.9	122	48.3	0.40
23	1.90	450	1420	26.5	–	355	1.85	761	0.286	14.0	201	0.200	42.8	76.1	57.4	0.75
24-A	0.263	245	3180	66.3	–	322	1.85	1220	0.125	29.8	390	0.182	133	177	38.6	0.22
24-B	0.451	584	3920	56.0	–	276	1.52	1560	0.179	38.0	431	0.218	93.6	188	73.9	0.39
25-A	0.363	512	897	23.1	–	152	2.30	446	0.430	20.4	78.0	–	36.1	34.4	383.0	11.12
25-B	0.501	601	769	17.4	2.84	141	2.04	409	0.304	19.0	72.1	–	31.9	32.1	226.9	7.06
25-C	–	116	824	17.6	0.646	147	2.52	436	0.394	20.1	75.3	–	34.1	34.5	266.5	7.72
25-D	–	65.5	873	6.78	–	155	2.63	465	0.340	25.4	81.0	–	39.0	36.4	335.2	9.21
25-E	0.238	213	838	12.4	–	144	2.30	441	0.358	18.2	75.2	–	33.8	33.6	284.7	8.46
25-F	0.476	683	700	26.7	–	126	2.89	360	0.573	15.9	62.4	–	24.4	32.6	113.3	3.47
25-G	0.989	985	734	26.3	1.36	134	2.59	378	0.412	20.3	67.2	–	27.2	33.0	129.4	3.92
26-A	–	10.9	1710	17.3	–	717	1.52	1050	0.286	18.7	280	–	64.0	64.6	62.5	0.97
26-B	–	28.3	1720	16.0	–	831	1.74	1070	–	20.4	283	0.055	66.2	65.3	56.2	0.86
26-C	–	97.3	1730	20.1	–	729	1.52	1080	–	18.1	284	0.036	67.4	67.5	54.4	0.81
26-D	–	21.2	1630	16.1	–	696	1.07	1020	0.233	18.8	269	–	62.6	62.1	52.8	0.85
26-E	–	11.3	1980	16.8	–	715	1.52	1050	0.143	18.8	275	–	65.1	65.1	55.9	0.86
26-F	–	55.1	1570	17.8	–	629	1.52	981	0.161	19.4	252	–	61.0	59.7	51.6	0.86
27	–	112	1430	11.9	–	67.7	–	534	0.197	7.70	211	0.273	38.2	65.8	64.3	0.98
28	–	5.78	1520	14.5	0.646	64.6	0.630	525	0.161	10.6	238	0.073	66.3	96.3	63.2	0.66
29	–	34.2	882	4.50	–	162	3.85	439	0.985	51.9	106	0.218	37.5	42.1	86.2	2.05
30	–	65.5	1960	28.6	1.23	878	0.741	1290	0.197	35.5	311	0.164	78.9	135	32.9	0.24
31	–	30.9	1170	9.57	–	431	1.11	764	0.430	22.3	171	0.291	49.4	165	44.1	0.27
32	–	37.7	1740	8.50	–	826	2.56	1050	0.519	42.4	437	0.237	72.4	134	47.6	0.36
33	–	29.4	1770	7.85	–	814	1.26	1040	0.555	43.6	424	0.473	69.2	134	42.1	0.31
34	–	6.09	1190	1.78	3.62	99.4	1.37	527	0.286	23.6	138	0.200	43.8	208	47.1	0.23
35	–	181	1350	6.93	–	569	2.63	828	1.36	38.1	278	0.218	45.7	89.6	54.7	0.61
36	–	113	1690	3.71	–	44.8	1.48	655	1.00	45.8	233	0.255	55.0	205	43.3	0.21
37	–	41.4	2060	3.57	3.71	29.8	1.67	681	3.60	50.2	327	0.837	93.7	208	66.2	0.32
38	–	154	1380	6.35	–	308	2.37	719	0.573	52.8	190	0.328	69.1	85.1	71.3	0.84
39	–	97.1	1220	3.71	–	442	4.67	690	0.967	38.4	264	0.218	92.9	160	111.1	0.69
40	–	197	1260	2.50	–	25.4	2.00	468	1.81	30.6	204	0.400	93.1	137	35.7	0.26
41	0.288	241	1230	1.86	2.07	29.6	1.63	465	0.412	36.8	181	0.491	126	27.2	7.4	0.27
42	–	26.4	1730	1.64	1.29	211	1.26	802	0.967	22.3	189	0.764	104	67.4	33.3	0.49
43-A1	–	3.70	499	2.36	1.49	260	5.74	411	1.33	17.1	62.3	0.146	23.6	27.6	36.0	1.30
43-A2	–	30.6	498	7.50	–	283	3.48	416	0.609	18.1	63.3	0.146	23.4	25.5	29.6	1.16
43-B	–	3.44	493	2.64	–	255	3.11	395	0.716	15.6	60.5	0.146	21.1	24.1	25.3	1.05
43-C	–	2.34	207	2.64	–	18.4	12.6	136	4.10	6.52	9.9	0.146	5.7	26.3	2.3	0.09
43-D	–	3.70	514	3.14	–	237	5.74	387	1.18	18.2	58.3	0.164	21.3	26.7	24.7	0.93
43-E	–	3.92	505	3.14	–	241	3.85	407	0.698	18.1	58.9	0.091	23.0	25.0	23.1	0.92
43-F	–	3.95	496	4.21	–	236	3.26	392	0.842	16.8	56.9	0.127	21.0	23.0	22.7	0.99
44	–	42.4	1040	9.07	–	476	3.37	696	0.412	19.9	147	0.400	94.9	63.1	49.3	0.78
45	–	98.4	2440	177	–	1770	2.37	1450	0.483	53.0	558	0.710	400	82.8	44.4	0.54
46	1.28	871	612	29.3	–	84.9	1.26	304	–	6.14	44.4	0.091	23.7	81.5	26.7	0.33
47	–	166	2940	209	–	320	2.00	1240	0.519	38.6	392	0.309	142	169	20.0	0.12
48	–	90.3	1240	7.85	–	221	3.11	549	0.609	25.0	180	0.328	77.3	59.2	112.8	1.90

[a]This sample was taken immediately downstream of the junction of the Copper River and the Kotsina River, and mixing between the two appears to be incomplete. This sample is therefore considered to reflect the Kotsina River and is excluded from further analyses.
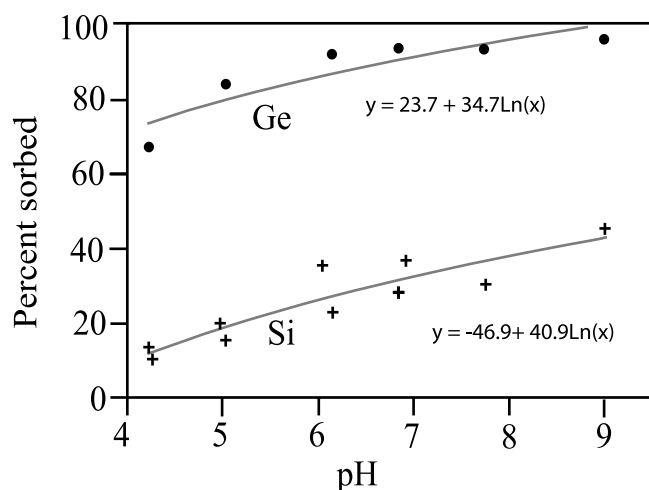
Figure 3. Sorption on hydrous iron oxides. The difference between measured concentrations of Si and Ge sample splits removed after contact with laboratory-precipitated hydrous iron oxides is shown as a function of pH. Loss of Ge and Si is due to sorption on the precipitate. The lines show log fits to the data. For Ge the r^2 value of the best fit semilog relation is 0.80; for Si, it is 0.83.

[14] Among the remaining rivers (Ge/Si $\leq$ 2 μmol/mol), significant differences between the glacial and periglacial basins exist: Ge/Si is higher in the glacial rivers (mean = 1.75, n = 28) than the periglacial rivers (mean = 0.57, n = 24) sampled (Table 3). The difference is significant at the 0.005 level according to a nonparametric Mann-Whitney test. In world rivers generally, high fluvial Ge/Si is associated with geomorphologically stable environments, thick, deeply weathered soil profiles, and warm and wet conditions [*Murnane and Stallard*, 1990; *Froelich et al.*, 1992]. However, the basins containing glacial rivers in the Copper River basin are less stable, and have less well developed soils than those of periglacial rivers, so the difference in Ge/Si between glacial and periglacial rivers does not show the same relationship to geomorphology that is seen in world rivers generally. Sulfide weathering is an unlikely cause of elevated Ge concentrations in these rivers because there is no correlation between Ge and S. Instead, other processes related specifically to glacial cover appear to influence Ge/Si.

[15] The fractions of Ge and Si sorbed on the hydrous iron oxide precipitated in our laboratory experiment are shown in Figure 3. These are calculated by measuring the Ge and Si concentration in the solution after contact with the precipitate and comparing them to the initial concentrations. In this laboratory experiment, the Ge is preferentially sorbed over Si by the hydrous iron oxide precipitated at room temperature at all pH values that were studied. As pH is increased, more Si and Ge are sorbed. However, the relative adsorption of Ge is approximately 7 times greater than for Si at slightly acid to neutral pH (Figure 3). At higher pH values, nearly all the Ge is sorbed while only about 1/3 of the Si is sorbed. The differential sorption changed the Ge/Si ratio of the solution from 2 μmol/mol before contact with

the precipitate to 0.79 μmol/mol at pH 4, decreasing to 0.15 μmol/mol at pH 9.

5. Discussion

[16] It is notable that the glacial and periglacial rivers sampled form distinct populations and that glacial rivers have higher Ge/Si ratios than periglacial rivers. A simple extrapolation from the results of this study to potential changes in global river chemistry due to the increased area of temperate glaciation during glacial periods would predict higher fluvial Ge/Si at the same time that the opal record of marine Ge/Si shows low ratios. This mismatch indicates that temperate glacial cover is not simply related to changes in marine Ge/Si. *Filippelli et al.* [2000] also note the opposite sense of variation of marine Ge/Si and their terrestrial record of Ge/Si over the past ~8000 years. However, marine Ge/Si requires some time to adjust to changes in the fluval inputs as the residence times of Ge and Si in the ocean are about 20,000 years [*Froelich et al.*, 1992]. In addition, the glaciers we studied in the Copper River region may not provide a good analogue to the continental ice sheets of the last glacial maximum. Nevertheless, the close correlation of Ge/Si with global ice volume [*Froelich et al.*, 1992] and our observed positive relationship between glacial cover and Ge/Si make a simple explanation of the marine Ge/Si record in terms of glacial cover impossible.

[17] The high Ge/Si ratios in glacial rivers and the low Ge/Si ratio in periglacial rivers both require explanation. We propose two mechanisms that may modify Ge/Si ratios in the Copper River Basin: (1) a disproportionate contribution from biotite weathering to subglacial streams creates a high Ge/Si ratio in glacial rivers and (2) a combination of differential sorption of Ge on hydrous iron oxides and preferential retention of Ge during clay mineral formation decreases the periglacial river Ge/Si below that of bedrock.

5.1. Biotite Weathering

[18] Silicate weathering accounts for relatively little of the dissolved load of subglacial streams [*Anderson et al.*, 1997]. *Drever and Hurcomb* [1986] found that biotite weathering surpasses feldspar weathering at South Cascade Glacier in northern Washington. Many researchers have observed that biotite, even when only a minor constituent of the bedrock, is the dominant silicate mineral to contribute to the subglacial dissolved load [*Blum et al.*, 1994; *Blum and Erel*, 1995; *Axtmann and Stallard*, 1995; *Anderson et al.*, 1997, 2000]. *Blum et al.* [1994] infer that biotite releases strontium about six times faster than K-feldspar in glaciated and recently (about 10,000 years ago) deglaciated basins in the Sierra Nevada. *Anderson et al.* [2000] also found biotite to be the principle subglacial silicate phase to weather chemically at the Bench Glacier in south central Alaska. Biotite weathering may dominate the subglacial silicate weathering signal because glacial erosion exposes fresh surfaces and biotite is physically susceptible to damage by glacial abrasion [*Nesbitt and Young*, 1996].

[19] High K/Na ratios are indicative of the contribution of biotite to the dissolved load of subglacial water [*Axtmann and Stallard*, 1995; *Stallard*, 1995; *Anderson et al.*, 1997]. In the Copper River Basin, high Ge/Si ratios in glacial rivers are correlated with high K/Na ratios (Figure 4 and Table 3).
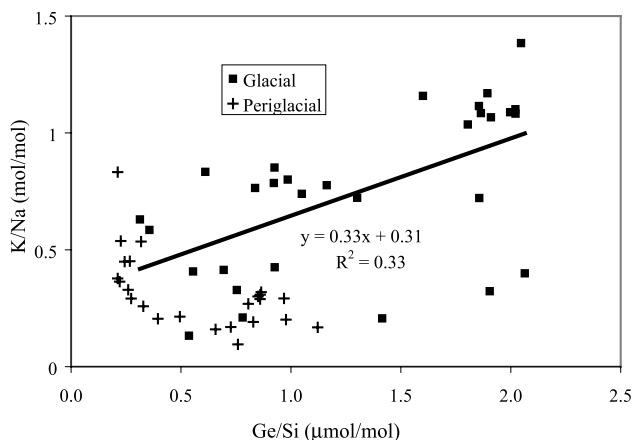
Figure 4. Ge/Si versus K/Na. The glacial rivers sampled have higher Ge/Si than periglacial rivers sampled and show a positive relationship between Ge/Si and K/Na. The linear trend is fitted to the glacial river data and is statistically significant (see text). Biotite has a high Ge/Si, and we suggest that the relation between Ge/Si and K/Na indicates biotite weathering can strongly influence the dissolved load chemistry in glacial systems. Periglacial rivers do not show a clear relationship between Ge/Si and K/Na.

The r^2 value of the linear correlation, 0.33, is significant at the 0.005 level in a standard normal linear correlation test (Figure 4). We suggest that the correlation of K/Na and Ge/Si in glacial rivers is due to the influence of biotite weathering on both ratios.

[20] Biotite is known to be enriched in Ge relative to most other silicate minerals and has a Ge/Si ratio of 3–4 times that of bulk continental crust [*Burton et al.*, 1959; *Filippelli et al.*, 2000; *Kurtz et al.*, 2002]. The incipient weathering reactions that release K and those that release Si and Ge are not the same since K (and Sr) are primarily released from the interlayer site in biotite, while Si (and Ge) are dominantly found in tetrahedral sites, with lesser quantities in octahedral sites. While we did not study the detailed reactions of biotite weathering, we note that several researchers have documented that the very early stages of biotite weathering are characterized by significant losses of Si as well as K [*Banfield and Eggleton*, 1988; *Pozzuoli et al.*, 1992; *Burkins et al.*, 1999]. This early loss of Si is likely to be accompanied by a loss of Ge at a Ge/Si greater than for most minerals even if some fractionation occurs. The observed correlation between Ge/Si and K/Na (Figure 4) is consistent with our hypothesis that biotite weathering influences Ge/Si as well as K/Na in glacial rivers. Our hypothesis is also consistent with the observations of *Filippelli et al.* [2000], who conclude that early weathering of biotite significantly increased fluvial Ge/Si ratios of a small alpine basin in southern California. In the glacial rivers, weak development of secondary alumino silicates (clays) that sequester Ge would limit fractionation by typical weathering processes.

5.2. Ge Sorption on Hydrous Iron Oxides

[21] The observation of low Ge/Si ratios in periglacial basins requires a change in either the source of Ge and Si, or active fractionation processes. We suspect that both factors are important in the Copper River Basin. First, it is likely that a wider variety of silicate minerals are weathering chemically in periglacial basins, diluting the effect of high Ge/Si biotite. Warm soils, humic acids, and more vegetation in the periglacial basins promote chemical alteration of silicate minerals. In addition, in the absence of glacial abrasion, biotite weathering rates in glacial sediment will decline, since new surfaces are not being exposed continuously. Glaciation does have a lasting impact on the chemistry of stream waters through the production of glacial sediment that can remain in the watershed long after deglaciation. *Blum et al.* [1994] found that in regions that have been glaciated in the last 10,000 years, the biotite is weathering 6 times faster than plagioclase weathering, about the same ratio as found for subglacial streams, while in basins that have not been glaciated in the past 100,000 years, biotite weathering is only 4 times faster than plagioclase weathering. *Anderson et al.* [2000] report a decreasing rate of biotite weathering with distance from the glacier terminus in the proglacial streams near the Bench glacier. We expect, therefore, that biotite weathering will remain disproportionately significant to the trace element concentration of the dissolved load for some time following deglaciation and gradually diminish with time. However, the Ge/Si ratio of many of the periglacial rivers is lower than that of common silicate minerals, indicating that congruent weathering of silicates cannot account for the low Ge/Si ratio and that a process must retain Ge in the soils.

[22] There are two proposed mechanisms for partitioning Ge into soils and out of the dissolved load: retention in clay minerals and sorption on iron oxides. Preferential inclusion of Ge in clay minerals is unlikely to have a significant effect in all of the periglacial basins because clay formation is may be limited due to the low temperatures and young soils in the steep and recently deglaciated basins. Unlike clay mineral formation, poorly crystalline iron oxides can accumulate rapidly in arctic soils and are early indicators of pedogenesis [*Ugolini*, 1986]. Iron oxides form from weathering of minerals and oxidation of sulfide minerals—reactions that occur rapidly even at low temperatures. Moreover, hydrous iron oxides are known to strongly, rapidly, and efficiently adsorb metals over a wide range of pH [*Benjamin et al.*, 1996]. Our laboratory experiments demonstrate that Ge is preferentially sorbed over Si on hydrous iron oxide precipitates, suggesting that Ge is likely to be preferentially sorbed on naturally occurring hydrous iron oxides in soils (Figure 3). Therefore sorption is a plausible mechanism for changing the Ge/Si ratio of streams without significant clay mineral formation and without large changes in the rates of biotite and plagioclase weathering. For these reasons, we favor preferential sorption on poorly crystalline iron oxides as an important control on Ge/Si ratios in periglacial rivers of the Copper River Basin.

[23] Our conclusion that differential sorption of Ge on iron oxides is likely to be an important control of Ge/Si ratios contrasts with that of *Chillrud et al.* [1994], who find the coexistence of a high Ge/Si ratio and pyrite oxidation in the glacial Upper Manso Stream in the Argentine Andes to be indirect evidence for a lack of control by iron oxide sorption. Nevertheless, two factors support sorption as a

potentially significant control on Ge/Si. First, pyrite itself can be significantly enriched in Ge [*Bernstein*, 1985], so much so that the net impact of subglacial pyrite oxidation may be to increase Ge/Si ratios even if preferential sorption is occurring. Secondly, the subglacial environment is quite distinct from a soil environment because of the limited contact of water with solid particles in the subglacial environment, implying that the sorption mechanism may be much more efficient in soil than in subglacial environments. However, our laboratory experiments do require cautious extension to the field results because naturally occurring iron oxides may differ in their surface area and sorption site density from the laboratory precipitate, and there are likely to be changes in the sorption potential over time [*Stumm*, 1992]. Clearly, a study of the amount and location of Ge and iron oxides in the soils of the Copper River Basin, as well as a study of the sorption of Ge and Si on naturally occurring hydrous iron oxides in conditions that mimic soil and subglacial environments is necessary to quantify the significance of this mechanism in controlling fluvial Ge/Si ratios. Our laboratory experiments suggest that preferential sorption of Ge on hydrous iron oxides is a viable mechanism for altering fluvial Ge/Si in our study area and motivate further study of the natural system.

[24] *Kurtz et al.* [2002] find that material removed by acid ammonium oxalate in the dark (AOD), including both allophane, a short range order aluminosilicate, and poorly crystalline Fe and Al oxides, accounts for the bulk of Ge sequestered in Hawaiian soils. They conclude that allophane is dominantly responsible for Ge/Si fractionation in the Hawaiian soils because Ge concentrations in the extracted material correlated well with Al and Si in the extractions, which is reasonable given that allophane is a dominant weathering product of ash-rich soils in both tropical and temperate regions. *Kurtz et al.* [2002] also note that all the weathering products they studied, including secondary clay minerals and crystalline iron oxides, have high Ge/Si ratios. This suggests that the dominant weathering products of a given soil determine the phase responsible for the bulk of Ge sequestration. Whether poorly crystalline hydrous iron oxides, or short-range order aluminosilicates like allophane, dominate the secondary oxides depends on the soil parent material; imogolite and allophane, occur in soils on volcanic material from tropical to temperate regions [*Ugolini and Dahlgren*, 1991], while hydrous iron oxides will likely dominate in nonvolcanic soils [*Schwertmann and Taylor*, 1989]. Changes in the soil mineralogy with time, especially the transition from poorly ordered to more crystalline aluminosilicates and Fe and Al oxides, may also partition Ge between different soil phases and the dissolved phase, and require more study.

6. Conclusions

[25] The marine record of Ge/Si cannot be interpreted as the direct result of changes in the extent of glaciers—as the simplest extrapolation from our observations would point to the opposite relationship between Ge/Si and glaciation than is observed in paleorecords. The global fluvial input of Ge and Si to the ocean reflects the dominant mineralogy of silicates being chemically weathered and the distribution and maturity of soils.

[26] Ge/Si ratios in runoff from extensively glaciated areas in the Copper River Basin are high relative to world rivers, as well as periglacial and recently deglaciated areas in the region. We suggest that these high ratios are due to biotite weathering. Several specific predictions can be made that could be tested with future research. First, the Ge/Si ratio in streams from other temperate glaciers should be elevated compared to local nonglacial basins, while Si concentrations will be low. Second, as biotite has both a high $^{87}Sr/^{86}Sr$ ratio and high Ge/Si, Ge/Si and $^{87}Sr/^{86}Sr$ should be positively correlated in subglacial waters.

[27] Additional research is needed to elucidate the processes partitioning Ge in diverse climatic regions. Meanwhile, we suggest that the relative importance of clay mineral formation and sorption on hydrous iron oxides varies with the maturity of the soils and the dominant mineralogy of the soil parent material in the basin. The model of fluvial Ge/Si from *Murnane and Stallard* [1990] pertains to late stages of soil development in warm climates with extensive weathering of secondary aluminosilicates and the release of sequestered Ge. However, for glacial and proglacial environments and for the young soils of recently deglaciated basins, further study is required to determine the relative importance of the two fractionation mechanisms. We suggest that sorption on hydrous iron oxides may be an important sequestration mechanism.

References

Anderson, S. P., J. I. Drever, and N. F. Humphrey, Chemical weathering in glacial environments, *Geology*, *25*, 399–402, 1997.

Anderson, S. P., J. I. Drever, C. D. Frost, and P. Holden, Chemical weathering in the foreland of a retreating glacier, *Geochim. Cosmochim. Acta*, *64*, 1173–1189, 2000.

Arnorsson, S., Germanium in Icelandic geothermal systems, *Geochim. Cosmochim. Acta*, *48*, 2489–2502, 1984.

Axtmann, E. V., and R. F. Stallard, Chemical weathering in the South Cascade Glacier basin, comparison of subglacial and extra-glacial weathering, in *Biogeochemistry of Seasonally Snow-Covered Catchments*, edited by K. A. Tonnessen et al., *IAHS-AISH Publ.*, *228*, 431–439, 1995.

Banfield, J. F., and R. A. Eggleton, Transmission electron microscope study of biotite weathering, *Clays Clay Miner.*, *36*(1), 47–60, 1988.

Bateman, A. M., and D. H. McLaughlin, Geology of the ore deposits of Kennicott, Alaska, *Econ. Geol.*, *15*, 1–80, 1920.

Benjamin, M. M., R. S. Sletten, R. P. Baily, and T. Bennett, Sorption and filtration of metals using iron-oxide-coated sand, *Water Res.*, *30*, 2609–2620, 1996.

Bernstein, L. R., Germanium geochemistry and mineralogy, *Geochim. Cosmochim. Acta*, *49*, 2409–2422, 1985.

Bernstein, L. R., and G. A. Waychunas, Germanium crystal chemistry in hematite and goethite from the Apex Mine, Utah, and some new data on germanium in aqueous solution and in stottite, *Geochim. Cosmochim. Acta*, *51*, 623–630, 1987.

Blum, J. D., and Y. Erel, A silicate weathering mechanism linking increases in marine 87Sr/86Sr with global glaciation, *Nature*, *373*, 415–418, 1995.

Blum, J. D., Y. Erel, and K. Brown, $^{87}Sr/^{86}Sr$ ratios of Sierra Nevada stream waters: Implications for relative mineral weathering rates, *Geochim. Cosmochim. Acta*, *58*, 5019–5025, 1994.

Blum, W. E. H., Arsenic in soils of Austria, final report, 94 pp., Inst. of Soil Sci., Univ. of Agric. Sci., Vienna, 1998.

Burkins, D. L., J. D. Blum, K. Brown, R. C. Reynolds, and Y. Erel, Chemistry and mineralogy of a granitic, glacial soil chronosequence, Sierra Nevada Mountains, California, *Chem. Geol.*, *162*, 1–14, 1999.

Burton, J. D., F. Culkin, and J. P. Riley, The abundances of gallium and germanium in terrestrial materials, *Geochim. Cosmochim. Acta*, *16*, 151–180, 1959.

Chillrud, S. N., P. F. Pedrozo, P. F. Temporetti, H. F. Planas, and P. N. Froelich, Chemical weathering of phosphate and germanium in glacial meltwater streams: Effects of subglacial pyrite oxidation, *Limnol. Oceanogr.*, *39*(5), 1130–1140, 1994.

Criaud, A., and C. Fouillac, Study of CO_2-rich thermomineral waters from the central French massif. 2. Behavior of some trace-metals, arsenic, antimony and germanium, *Geochim. Cosmochim. Acta*, *50*, 1573–1582, 1986.

Drever, J. I., and D. R. Hurcomb, Neutralization of atmospheric acidity by chemical weathering in an alpine drainage basin in the North Cascade Mountains, *Geology*, *14*, 221–224, 1986.

Dzombak, D. A., and F. M. M. Morel, *Surface Complexation Modeling: Hydrous Ferric Oxide*, 393 pp., John Wiley, Hoboken, N. J., 1990.

Elderfield, H., and A. Schultz, Mid-ocean ridge hydrothermal fluxes and the chemical composition of the oceans, *Annu. Rev. Earth Planet. Sci.*, *24*, 191–224, 1996.

Emery, P. A., S. H. Jones, and R. L. Glass, Water resources of the Copper River Basin, Alaska, in *Hydrologic Investigations Atlas HA-686*, 3 sheets, U.S. Geol.Surv., Reston, Va., 1985.

Evans, M. J., and L. A. Derry, Ge/Si ratios as a tracer of hydrothermal activity in the Nepal Himalaya, *Eos Trans. AGU*, *82*(47), Abstract V41C-08, 2001.

Evans, M. J., and L. A. Derry, Quartz control of high germanium-silicon ratios in geothermal waters, *Geology*, *30*, 1019–1022, 2002.

Filippelli, G. M., J. W. Carnahan, L. A. Derry, and A. Kurtz, Terrestrial paleorecords of Ge/Si cycling derived from lake diatoms, *Chem. Geol.*, *168*, 9–26, 2000.

Froelich, P. N., G. A. Hambrick, M. O. Andreae, R. A. Mortlock, and J. M. Edmond, The geochemistry of inorganic germanium in natural waters, *J. Geophys. Res.*, *90*, 1133–1141, 1985.

Froelich, P. N., V. Blanc, R. A. Mortlock, and S. N. Chillrud, River fluxes of dissolved silica to the ocean were higher during glacials: Ge/Si in diatoms, rivers and oceans, *Paleoceanography*, *7*(6), 739–767, 1992.

Hammond, D. E., J. McManus, W. M. Berelson, C. Meredith, G. P. Klinkhammer, and K. H. Coale, Diagenetic fractionation of Ge and Si in reducing sediments: The missing Ge sink and a possible mechanism to cause glacial/interglacial variations in oceanic Ge/Si, *Geochim. Cosmochim. Acta*, *64*, 2453–2465, 2000.

King, S. L., P. N. Froelich, and R. A. Jahnke, Early diagenesis of germanium in sediments of the Antarctic South Atlantic: In search of the missing Ge sink, *Geochim. Cosmochim. Acta*, *64*, 1375–1390, 2000.

Kurtz, A. C., Germanium/silicon and trace element geochemistry of silicate weathering and mineral aerosol deposition, Ph.D. thesis, 186 pp., Cornell Univ., Ithaca, N. Y., 2000.

Kurtz, A. C., L. A. Derry, and O. A. Chadwick, Germanium-silicon fractionation in the weathering environment, *Geochim. Comsochim. Acta*, *66*, 1525–1537, 2002.

Miller, T. P., Geothermal resources of Alaska, in *The Geology of North America*, vol. G1, *The Geology of Alaska*, edited by G. Plafker and H. C. Berg, p. 979–987, Geol. Soc. of Am., Boulder, Colo., 1994.

Mortlock, R. A., and P. N. Froelich, Continental weathering of germanium: Ge/Si in the global river discharge, *Geochim. Cosmochim. Acta*, *51*, 2075–2082, 1987.

Mortlock, R. A., and P. N. Froelich, Determination of germanium by isotope dilution-hydride generation inductively coupled plasma mass spectrometry, *Anal. Chim. Acta*, *332*, 277–284, 1996.

Mortlock, R. A., P. N. Froelich, R. A. Feely, G. J. Massoth, D. A. Butterfield, and J. E. Lupton, Silica and germanium in Pacific Ocean hydrothermal vents and plumes, *Earth Planet. Sci. Lett.*, *119*(3), 365–378, 1993.

Motyka, R. J., R. J. Poreda, and A. W. A. Jeffrey, Geochemistry, isotopic composition, and origin of fluids emanating from mud volcanoes in the Copper River basin, Alaska, *Geochim. Cosmochim. Acta*, *53*, 29–41, 1989.

Munhoven, G., and L. M. Francois, Glacial-interglacial variability of atmospheric CO_2 due to changing continental silicate rock weathering: A model study, *J. Geophys. Res.*, *101*, 21,423–21,437, 1996.

Murnane, R. J., and R. F. Stallard, Germanium and silicon in rivers of the Orinoco drainage basin, *Nature*, *344*, 749–752, 1990.

Nesbitt, H. W., and G. M. Young, Petrogenesis of sediments in the absence of chemical weathering: Effects of abrasion and sorting on bulk composition and mineralogy, *Sedimentology*, *43*, 341–358, 1996.

Nokleberg, W. J., G. Plafker, and F. H. Wilson, Geology of south-central Alaska, in *The Geology of North America*, vol. G1, *The Geology of Alaska*, edited by G. Plafker and H. C. Berg, pp. 311–366, Geol. Soc. of Am., Boulder, Colo., 1994.

Pozzuoli, A., E. Vila, E. Franco, A. Ruiz-Amil, and C. De La Calle, Weathering of biotite to vermiculite in Quaternary lahars from Monti Ernici, central Italy, *Clay Miner.*, *27*, 175–184, 1992.

Schwertmann, U., and R. M. Taylor, Iron oxides, in *Minerals in Soil Environments*, SSSA Book Ser., vol. 1, edited by J. B. Dixon and S. B. Weed, pp. 379–438, Soil Sci. Soc. of Am., Madison, Wisc., 1989.

Stallard, R. F., Relating chemical and physical erosion, in *Chemical Weathering Rates of Silicate Minerals*, *Rev. Mineral.*, vol. 31, edited by A. F. White and S. L. Brantley, pp. 543–564, Mineral. Soc. of Am., Washington, D. C., 1995.

Stumm, W., *Chemistry of the Solid-Water Interface: Processes at the Mineral-Water and Particle-Water Interface in Natural Systems*, 428 pp., John Wiley, Hoboken, N. J., 1992.

Ugolini, F. C., Pedogenic zonation in the well-drained soils of the arctic regions, *Quat. Res.*, *26*, 100–120, 1986.

Ugolini, F. C., and R. A. Dahlgren, Weathering environments and occurrence of imogolite/allophane in selected Andisols and Spodosols, *Soil Sci. Soc. Am. J.*, *55*(4), 1166–1171, 1991.

Zhou, L., and F. T. Kyte, Are there any significant sinks in the marine Ge cycle other than biogenic opal?, *Eos Trans. AGU*, *72*(45), Fall Meet. Suppl., 263–264, 1991.

————————————

A. M. Anders, Department of Earth and Space Sciences, University of Washington, Box 351310, Seattle, WA 98195-1310, USA. (andersa@u.washington.edu)

L. A. Derry, Department of Earth and Atmospheric Sciences, Cornell University, 4142 Snee Hall, Ithaca, NY 14853-4780, USA. (lad9@cornell.edu)

B. Hallet and R. S. Sletten, Quaternary Research Center, University of Washington, Box 351360, Seattle, WA 98193-1360, USA. (hallet@u.washington.edu; sletten@u.washington.edu)